

# The EUSO Mission

Jim Adams<sup>a</sup> for the EUSO Consortium

<sup>a</sup>Mail Code SD50, NASA Marshall Space Flight Center, Huntsville, AL 35812, USA

The investigation of cosmic rays with energies in excess of  $10^{20}$  eV holds the potential for discoveries in astrophysics, cosmology and/or fundamental physics. This has motivated the construction of very large ground-based experiments and has lead to the development of the first space mission to measure these cosmic rays, the Extreme Universe Space Observatory (EUSO). EUSO will use the Earth's atmosphere viewed from space as a detector of extreme energy cosmic rays (EECRs). EUSO's collecting power will exceed the present experiments by more than a factor of 10 and extend the cosmic ray spectrum beyond 100 EeV with high statistics.

## 1. BACKGROUND

Following the discovery of the cosmic microwave background (CMB) by Penzias and Wilson<sup>1</sup> in 1965, Greisen<sup>2</sup> and Zatsepin and Kuz'min<sup>3</sup> predicted in 1966 that pions would be produced by the interaction of the CMB with cosmic rays above  $\sim 5 \times 10^{19}$  eV, robbing these cosmic rays of their energy so that only cosmic rays from sources  $< 100$  Mpc distant would arrive at earth above  $10^{20}$  eV. This is nearby on the scale of the Universe. As a result, it was anticipated that the cosmic ray spectrum would end by  $10^{20}$  eV but on the 15<sup>th</sup> of October, 1991 the Fly's Eye experiment<sup>4</sup> recorded an event with  $3.2 \times 10^{20}$  eV. Since 1991 the form of the cosmic ray spectrum above  $10^{20}$  eV as well as the origin and the nature of the particles themselves have remained uncertain.

### 1.1. Previous measurements

Since 1991 cosmic rays with energies in excess of  $10^{20}$  eV have been reported by every instrument with enough collecting power to observe them. Figure 1<sup>5</sup> shows the spectra measured by Fly's Eye, AGASA, HiRes1 and HiRes2. While Fly's Eye, AGASA and HiRes1 have observed cosmic rays with energies in excess of  $10^{20}$  eV, the HiRes1 spectrum is noticeably below the one reported by AGASA but this discrepancy may not be statistically significant<sup>6</sup>.

### 1.2 Present measurements

The Fly's Eye and AGASA experiments have now been completed but HiRes (High Resolution Fly's Eye) continues to operate, so we can expect additional data. HiRes1 and 2 are designed to operate together to obtain stereo images of extensive air showers<sup>7,8</sup>. This will make it possible to determine the range by triangulation and provide redundant measurements along different paths in the intervening atmosphere. These redundant 571814 measurements should reveal any deficiencies in the corrections for atmospheric losses (mainly from aerosols in the planetary boundary layer).

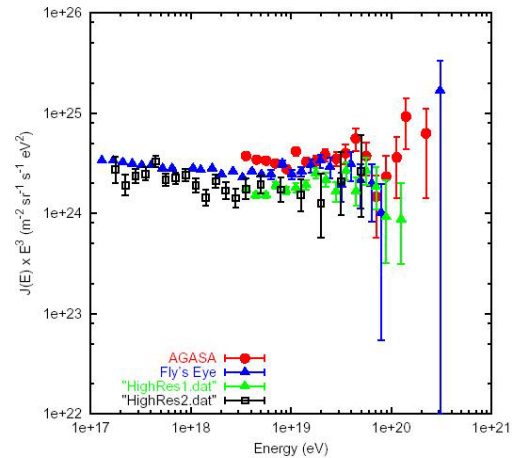


Figure 1: The ultrahigh energy cosmic ray spectral data from: the analysis of Fly's Eye observations (dark triangles), AGASA (circles), HiRes I-monocular (light triangles), and HiRes II-monocular (squares). This figure is taken from Stecker<sup>5</sup>.

The next generation ground-based experiment is already coming on-line. When it is complete, the Pierre Auger Southern Observatory<sup>9,10,11</sup> will cover 3000 km<sup>2</sup> near Malargue, Argentina and have a geometry factor of 7400 km<sup>2</sup>sr. This is a hybrid instrument consisting of both a ground array and a fluorescent detector system which is expected to simultaneously measure ~10% of the events.

The Pierre Auger Observatory (PAO) is expected to have an energy resolution of 12% and an angular resolution of 0.6° (10% and 0.5° when simultaneous fluorescent measurements are made). The PAO is expected to be capable of separating photons from hadrons on an event-by-event basis<sup>12</sup>. Simulations also demonstrate that good separation between protons and iron can be obtained using an artificial neural network, especially when data from the air fluorescence measurements are included<sup>12</sup>.

Neutrino ( $\nu$ ) detection with the PAO is expected to be difficult<sup>13</sup>. The ground array is potentially capable of detecting  $\nu$ s interacting in the atmosphere with zenith angles  $>80^\circ$  but the only detectable signal may come from nearly horizontal  $\nu_\tau$ s that skim the earth, producing  $\tau$ s that decay over the array<sup>14</sup> but the sensitivity is above the Waxman-Bachall upper bound<sup>15</sup>. The PAO fluorescence detector also has the capability to detect  $\nu$ s, but the detection efficiency is quite small<sup>16</sup>.

## 2. EUSO

Extending the cosmic ray spectrum beyond 10<sup>20</sup> eV with high statistical precision requires such large collecting areas that the next generation of experiments must be space-based. The first of these will be the Extreme Universe Space Observatory (EUSO).

### 2.1 The EUSO Experiment

EUSO, shown in figure 2, is very large wide angle UV camera that will be located on the Columbus module of the International Space Station. This focal surface is populated with multi-anode photo-multiplier tubes that operate in single photon counting mode.

From its berth on the ISS, EUSO views a large area in the atmosphere below. An extensive air shower (EAS) initiated by an EECR appears as a thin

luminous disk streaking down though the atmosphere at the speed of light. Operating as a high-speed movie camera, EUSO records a video clip of the progress of the EAS shower front and the reflected Čerenkov flash from its footprint at the earth.

Because EUSO uses the atmosphere as its detector, it must be equipped with an atmospheric sounding (AS) system to measure the atmospheric conditions both along the path of the EAS and within the column of atmosphere through which that path was viewed so that the measurements can be corrected for losses due to scattering and absorption.

To optimize the signal-to-noise ratio, EUSO observes in the 330-400 nm band which contains several strong nitrogen fluorescent lines just above the atmospheric cutoff. Optical filters on the focal surface are used to define the upper end of this band.

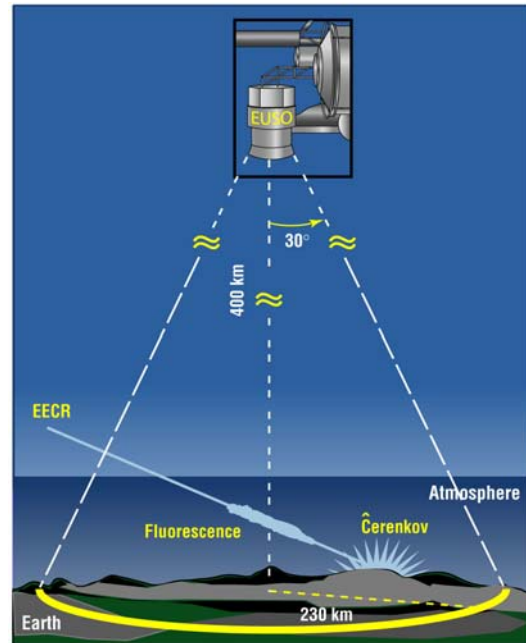


Figure 2: EUSO uses the Earth's atmosphere as its detector. Within its wide field of view, EUSO records both the fluorescence and the reflected Čerenkov light from an EAS.

Figure 3 shows the differential acceptance,  $d\Omega/d\theta$ , of EUSO as a function of the zenith angle,  $\theta$ , of the EECR. The differential geometrical acceptance is

proportional to  $\sin\theta\cos\theta$ . The figure also shows the results of detailed numerical simulations of the performance of EUSO for  $10^{20}$  eV proton EECRs that shows the differential acceptance for events recorded by EUSO. For 80% of the events, both the fluorescent and the Čerenkov signal are observed. The fluorescent signal only is observed for an additional 11% of the event. These events are still useful in the data analysis so the overall detection efficiency is 91% for an effective acceptance of  $550,000 \text{ km}^2 \text{ sr}$ .

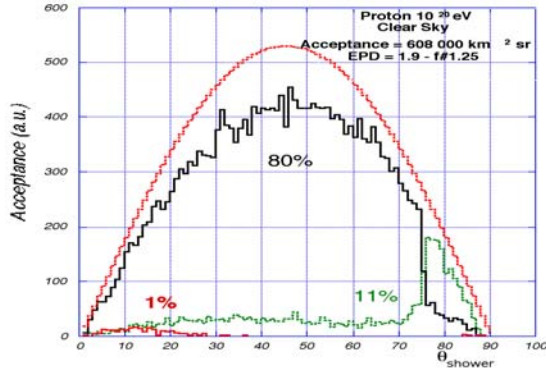


Figure 3: This figure shows the differential acceptance of EUSO (in arbitrary units) versus the zenith angle of the EECR. The top curve is the differential geometrical acceptance. Also shown are the results of numerical simulations showing the differential acceptance for those events in which only the fluorescent signal was observed (11%), only the Čerenkov signal was observed (1%) and both were observed (80%).

EUSO makes its measurements by viewing the nighttime atmosphere when the ISS is in umbra (34% of the time). EUSO must also have low moonlight conditions (50-75% of the time). In addition, EUSO cannot make measurements where city lights are in the background. All together, the observing duty factor for EUSO is ~17-25% of the time.

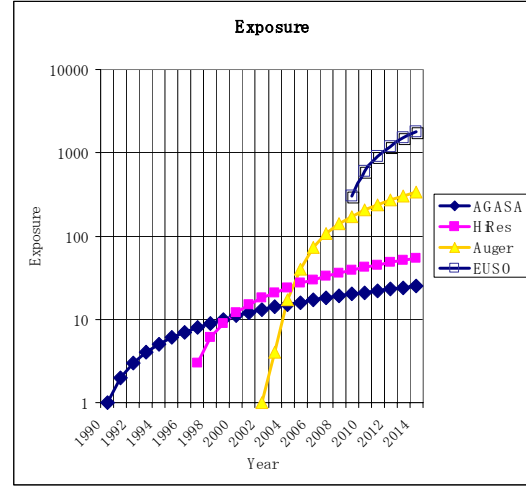


Figure 4: This figure shows how the exposure increases with time for EUSO compared to Auger, HiRes and AGASA (*should it have continued operation*).

Clouds can also interfere with measurements and they are present about 66.5% of the time, but 2/3 of these are at low altitudes below the maxima of the EASs that EUSO is observing.

Using its AS system, EUSO can measure the altitude of these low-lying clouds and use the Čerenkov reflection from them as the shower footprint. In all, we expect to make measurements about 15% of the time so that the effective geometry factor for EUSO is approximately  $80,000 \text{ km}^2 \text{ sr}$ . Figure 4 shows how the exposure of EUSO will increase with time in comparison with the other experiments where the exposure,  $E$ , is defined as

$$E = \int_0^t \Omega dt'.$$

It is clear that the exposure accumulated during the EUSO mission will exceed those of other experiments by a large factor.

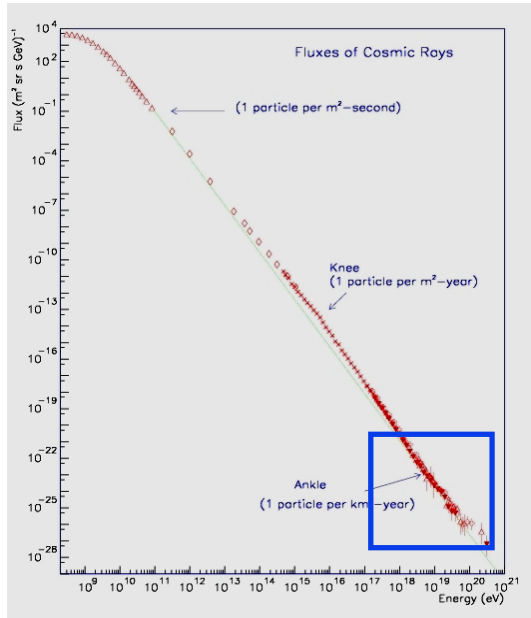


Figure 5: The cosmic ray all particle spectrum showing the locations of the “knee” and the Ankle (taken from Swordy<sup>17</sup>).

Figure 6 compares EUSO’s statistical precision to that of existing experiments, assuming that the cosmic ray spectrum continues above  $10^{20}$  eV as a power law with a spectral index of -3. In this case EUSO will extend measurements of the spectrum well beyond  $10^{21}$  eV.

## 2.2 The principal science goal of EUSO

Figure 5 shows the all particle cosmic ray spectrum.<sup>17</sup> Its form above  $10^{10}$  eV is an almost featureless power law. There is a slight steepening at around  $10^{16}$  eV called the “knee” and a small flattening near  $10^{18}$  eV called the “ankle”. Up to the “ankle” cosmic rays are thought to be of galactic origin. Above  $10^{18}$  eV it is thought that the Larmor radius of protons in the Galactic magnetic fields is such that cosmic rays can no longer be confined to the Galaxy<sup>18</sup>. Indeed, it has been found<sup>19</sup> that below the “ankle” cosmic rays arrival directions have anisotropy toward the Galactic center, but above the “ankle” they are isotropic, indicating that these cosmic rays are extragalactic. Beyond  $5 \times 10^{19}$  eV protons are expected to lose energy by pion production on the microwave background (called the GZK cutoff). If the cosmic ray spectrum continues far above this energy (as appears to be the case), we

should expect the composition of the cosmic rays to change.

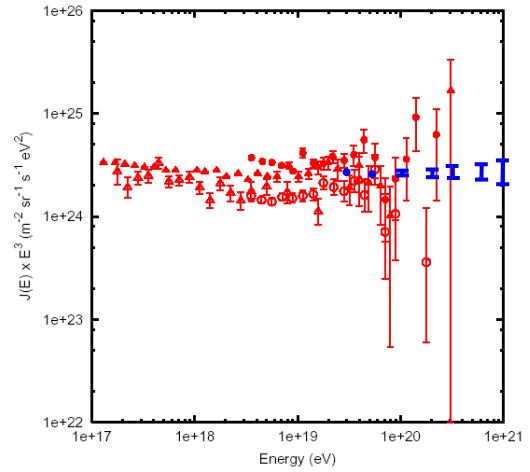


Figure 6: This figure shows the existing data (taken from Stecker<sup>5</sup>) with simulated data from EUSO superimposed.

As Hillas<sup>18</sup> argues, above  $10^{20}$  eV it becomes increasingly difficult to conceive of mechanisms that can accelerate cosmic rays in any known astrophysical objects, so above this energy even the source of cosmic rays may be different.

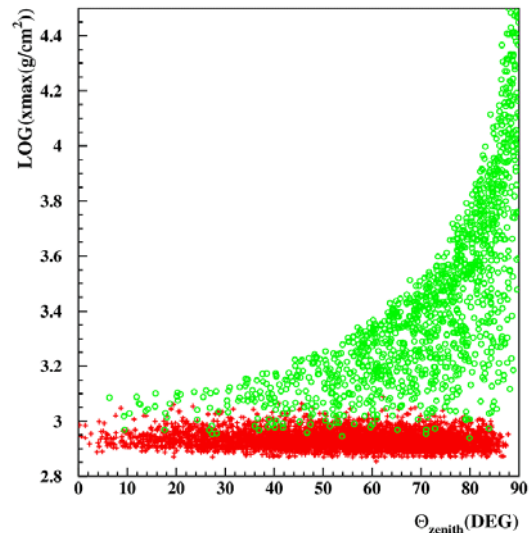


Figure 7: This figure shows how hadron-initiated showers (+s) and neutrino-initiated showers (o) can be distinguished when the depth of shower maximum can be measured.

The science driver for the EUSO mission is the investigation of the highest energy processes present and accessible in the Universe through the detection and analysis of the extreme energy component of the cosmic radiation (i.e. particles with energies  $> 5 \times 10^{19}$  eV). In this investigation we will attempt to answer the question “Where do the ultrahigh-energy cosmic rays come from?”, one of the 11 greatest unanswered questions in physics<sup>20</sup>.

### 2.1. Neutrino detection

Above  $\sim 10^{20}$  eV the Universe is expected to be transparent only to neutrinos. The second science goal of EUSO is to open the channel of ultra high energy neutrino astronomy to probe the boundaries of the extreme universe and to investigate the nature and distribution of the EECR sources.

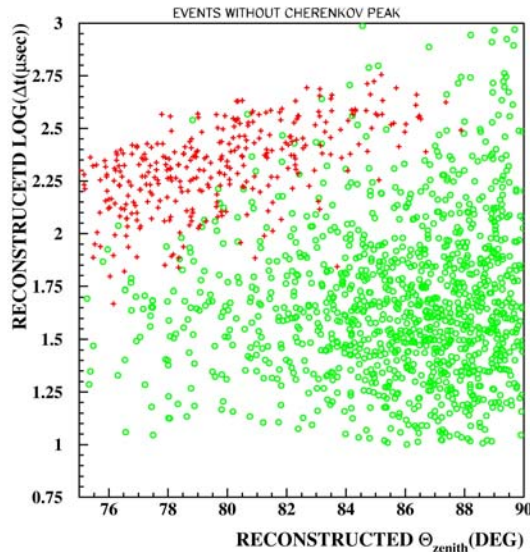


Figure 8: This figure shows that hadron-initiated showers (+’s) and neutrino-initiated showers (o’s) can be distinguished even when the Čerenkov flash is not seen.

As figure 7 shows, we can separate showers initiated by hadrons and neutrinos almost always on an event by event basis for those events in which we record both the fluorescent and the Čerenkov signals, allowing us to measure the location of the shower maximum in  $\text{g/cm}^2$ . As shown in figure 3, this applies to 80% of the proton-initiated shower at  $10^{20}$  eV. For another 11%, mostly at large zenith angles, it was only possible to measure the fluorescent signal. As figure 8 shows, neutrino- and hadron-

initiated showers can also be distinguished at large zenith angles when only the fluorescent signal is available.

Because EUSO tracks the EAS shower front through the atmosphere, it can determine the arrival direction of the cosmic ray, typically to an accuracy of  $0.2^\circ$ . This makes it possible to do astronomy with both neutrino and hadron cosmic rays. In the case of charged cosmic rays, the angular resolution will be limited by the intergalactic magnetic fields probably to  $\sim 2^\circ$ .

### 2.2. Detection of gamma-rays and nuclei

EUSO also is capable of distinguishing showers initiated by protons, heavier nuclei and gamma rays as shown in figure 9. Because of the dispersion in the depth of the first interaction, it is not possible to separate protons from iron nuclei and gamma rays event by event, but they can be separated on a statistical basis.

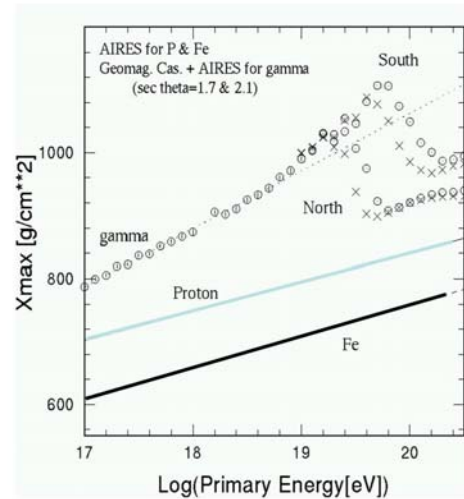


Figure 9: This figure shows ARIES calculations of the depth of shower maximum versus energy for showers initiated by gamma rays, protons and Iron nuclei.

## 3. INVESTIGATIONS

In this section we examine the theoretical predictions for the spectra and the nature and sources of EECRs. We show that EUSO has the capability to test the predictions of most of these models. Models for cosmic ray acceleration have been recently reviewed by Stecker<sup>5</sup> and Olinto<sup>24</sup>.



### 3.1 GZK proton spectra

Figure 10 shows four models of the EECR spectrum in case EECRs are protons and obey the GZK cutoff. Also indicated by the diagonal line is where a data point constructed from the four highest energy EUSO events would be plotted. It's clear that EUSO has the possibility not only to confirm the GZK cutoff but also to distinguish between most of these models.

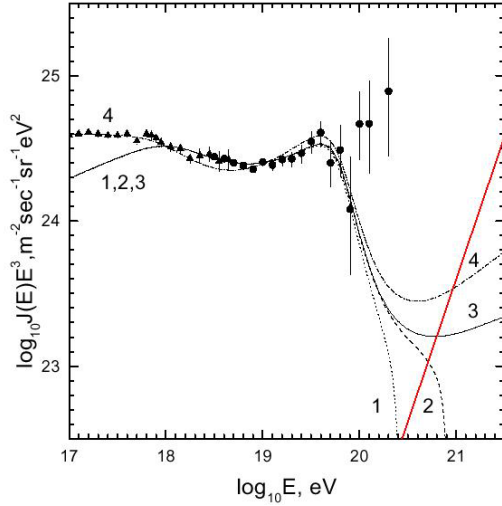


Figure 10: Shown in this figure (taken from Berezhenski<sup>21</sup>) are AGASA measurements<sup>22</sup> along with calculations of the GZK cutoff. For curves 1, 2, and 3 the source spectrum was assumed to be  $E^{-2.7}$  and cosmological evolution was neglected. The cutoff energies of the source spectra were assumed to be  $2 \times 10^{20}$  eV,  $10^{21}$  eV and  $\infty$ . Curve 4 assumes a source spectrum of  $E^{-2.45}$  that extends to  $\infty$  and cosmological evolution according to  $(1+z)^4$ . A data point constructed from the four highest energy events recorded by EUSO would be plotted somewhere along the diagonal line.

The cosmic rays above  $10^{20}$  eV could be heavier nuclei. This would shift the GZK cutoff to  $5A \times 10^{19}$  eV, where  $A$  is the atomic mass. In the case of Fe, the GZK cutoff would be  $2.8 \times 10^{22}$  eV. However before Fe nuclei reach this energy, they will photodisintegrate through interactions with the photon background, principally the CMB<sup>23</sup>. Above  $2 \times 10^{20}$  eV photodisintegration destroys Fe nuclei from source farther than a few Mpc.

One is led to conclude that hadronic EECRs with energies  $> 2 \times 10^{20}$  eV must come from nearby sources.

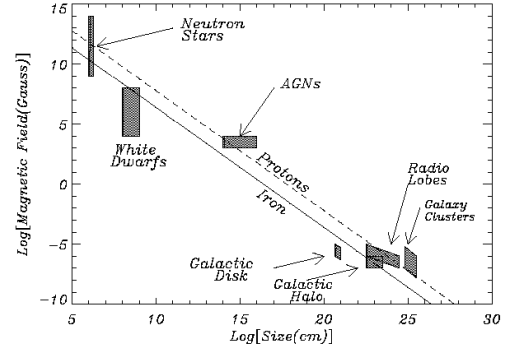


Figure 11: This plot originally due to Hillas<sup>18</sup> has been revised by Olinto<sup>24</sup>. It shows the magnetic field needed to confine cosmic rays while they are accelerated to EECR energies depending on the scale-size of the confinement region. The positions of various candidate accelerators are plotted. The diagonal lines correspond to requirements for accelerating iron and protons to  $10^{20}$  eV assuming that shock speeds are  $\beta=1$ .

### 3.2 Bottom-up source candidates

Hillas<sup>18</sup> has examined the conditions required for the acceleration of EECRs (see figure 11). He concludes that protons cannot be accelerated beyond  $10^{20}$  eV by any known astrophysical object even if the accelerating shocks are propagating at the speed of light. For more realistic shock speeds of  $\beta=1/300$ , not even Fe nuclei can be accelerated to energies beyond  $10^{20}$  eV.

So one is lead to conclude that hadronic cosmic rays beyond  $\sim 2 \times 10^{20}$  eV must come from local sources, but no known astrophysical objects, near or far, appear to be capable of accelerating hadronic cosmic rays to these energies.

### 3.3 Top-Down Candidates

From the conclusion above, we are lead to suspect that the sources of EECRs above  $2 \times 10^{20}$  eV are objects about which we now know nothing!

This has lead to extensive speculation and many hundreds of papers suggesting possible sources, many of which depend on the existence of yet-to-be discovered particles or physical principles. These

include topological defects, Z-bursts and heavy dark matter particles called “wimpzillas”.

The reader is referred to the reviews by Stecker<sup>5</sup> and Olinto<sup>24</sup> for a detailed discussion of both “bottom-up” acceleration models and “top down” models.

Table 1: A truth table showing the tests that EUSO can perform and how these tests can be used to distinguish between various models EECRs.

EUSO Test	GRB	AGN	TD	Wimpzillas	Z-Burst	$P_{\gamma_{2.7K}}$ neutrinos	Quantum Gravity	LI Violation
<i>Coincidence with GRB</i>	X	-	-	-	-	-	-	-
$(N_o/N_p) \gg 1$	-	-	X	X	X	X	-	-
$(N_o/N_p) > 1$	X	-	X	X	X	-	X	-
<i>Anisotropy</i>	-	-	-	X	X	-	-	-
<i>Multiple events</i>	X	X	-	-	X	-	-	X
<i>Distant Point Sources</i>	-	-	-	-	-	-	-	X
<i>Nearby Point Sources</i>	-	X	-	-	-	-	-	-
<i>After GRB</i>	-	-	-	-	-	-	X	-
<i>Cutoff Energy</i>	X	X	-	-	$10^{20}$ eV/ $m_0$	X	X	-

### 3.4 Other new physics

New physical processes, waiting to be discovered, may be responsible for EECRs (see Stecker<sup>5</sup> and papers referenced within). Two interesting suggestions are described briefly below.

Present estimates are that neutrinos have a probability of  $\sim 10^{-5}$  of interacting in  $1000 \text{ g/cm}^2$  of air at  $10^{19} \text{ eV}$ <sup>15</sup> and somewhat more at higher energies. There may be a large increase in the neutrino cross section at EECR energies thus increasing the probability that they will interact in the atmosphere.

Violations of Lorentz invariance have also been suggested as a way to avoid the GZK cutoff, allowing cosmic ray hadrons to arrive from great distances.

It is expected that gamma rays in the range  $10^{13} - 10^{20} \text{ eV}$  are attenuated by pair production on infrared, microwave, and radio backgrounds, therefore, no gammas from distant sources are expected. It has been conjectured<sup>25</sup> that quantum gravity effects may make the universe transparent to such gamma rays. EUSO observations of EECR gamma rays originating from distant sources would be evidence for this effect. Some quantum gravity theories<sup>26</sup> suggest that the speed of light ( $c$ ) is reduced for very high-energy gamma rays. EUSO could observe this effect by a time delay between a gamma-ray burst and the arrival of the high-energy gamma rays.

### 3.5 Distinguishing between the models

Stecker<sup>5</sup> has compiled a table showing the tests that could distinguish between the models. That table is reproduced and amended here as Table 1. It shows how EUSO measurements can be used to discriminate between various proposed models for EECRs. Most models can be distinguished by using spectral measurements, timing, multiple event detection capability, pointing accuracy, and composition measurements that EUSO can make. This table demonstrates the discovery potential of EUSO.

## 4. THE ORBITING WIDE ANGLE LIGHT COLLECTOR

If EUSO is successful it will give us our first clear definition of the cosmic ray spectrum extending up to  $10^{21} \text{ eV}$ . EUSO is capable testing the theories discussed above and making discoveries about the nature of extreme energy cosmic rays and their sources. If EUSO does make exciting discoveries, the case for extending the investigations with even better statistics will be compelling. A mission to follow EUSO is already in planning. This is the Orbiting Wide Angle Light Collector (OWL)<sup>27</sup>. OWL consists of two satellites that will fly in formation to provide a stereo view of the detector volume in the atmosphere. It is expected to have an angular resolution of  $0.2^\circ$  and an energy resolution

of 14%. The effective geometry factor will be  $2.3 \times 10^5 \text{ km}^2 \text{ ster.}$ ,  $\sim 2.8$  times larger than EUSO.

## 5. CONCLUSIONS

The Extreme Universe Space Observatory will extend measurements of the cosmic ray spectrum a decade higher in energy, entering an energy range where both the composition of cosmic rays and the nature of their sources probably will change. EUSO has the capability to measure the composition and arrival direction of these EECRs, giving it the potential to make important discoveries in astrophysics, cosmology and/or fundamental physics.

## 6. ACKNOWLEDGEMENTS

The authors would like to thank Dr. Robert Streitmatter of GSFC for contributing information on the OWL mission and Dr. Floyd Stecker for assistance with the figure 1. This work was supported in the US by the Explorer Program Office of NASA's Office of Space Science.

## REFERENCES

1. Penzias, A.A. and Wilson, R.W. (1965), *Astrophys. J.* **142**, 419.
2. Greisen, K. (1966) *Phys. Rev. Letters* **16**, 748.
3. Zatsepin, G.T. and Kuz'min, V.A. (1966), *Zh. Eks. Teor. Fiz., Pis'ma Red.* **4**, 144.
4. Bird et al.
5. Stecker, F. W. (2003), *J. Phys. G: Nucl. Part. Phys.* **29**, R47-R88.
6. De Marco, D., Blasi, P. and Olinto, A.V (2003), *Astroparticle Phys.*, in press, astro-ph/0301497.
7. Archbold, G. and Sokolsky, P.V. (2003), 28<sup>TH</sup> ICRC, (Universal Academy Press, Inc., Tokyo).
8. Springer, R. Wayne et al. (2003), 28<sup>TH</sup> ICRC, (Universal Academy Press, Inc., Tokyo).
9. Dova, T. et al. (2001), 27<sup>TH</sup> ICRC, (Copernicus Gesellschaft, Hamburg), 699.
10. Lloyd-Evans, J. et al. (2001), 27<sup>TH</sup> ICRC, (Copernicus Gesellschaft, Hamburg) 707.
11. Cester, R. et al. (2001), 27<sup>TH</sup> ICRC, (Copernicus Gesellschaft, Hamburg) 711.
12. Medina-Tanco, G. and Sciutto, S. (2001), 27<sup>TH</sup> ICRC, (Copernicus Gesellschaft, Hamburg) 1.
13. Ave, M., Vazquez, R., Zas, E. (2000), *Astropart. Phys.* **14** 109.
14. Letessier-Selvon et al. (2001), 27<sup>TH</sup> ICRC, (Copernicus Gesellschaft, Hamburg) 722.
15. Wilczynski, H. (2000), *Acta Physica Polonica B*, **31**, 1403
17. <http://hep.uchicago.edu/~swordy/crspec.html>
16. Guerard, C. (2001), 27<sup>TH</sup> ICRC, (Copernicus Gesellschaft, Hamburg) 760.
18. Hillas, A.M. (1984) *Ann. Rev. Astron. Astrophys.*, **22**, 425.
19. Hayashida, N. et al. (1999), *Astroparticle Phys.* **10**, 303.
20. Turner, M. et al (2003) "Connecting Quarks with the Cosmos: Eleven Science Questions for the New Century", National Academy Press, (Washington).
21. Berezensky et al. (2002), hep-ph/0204357.
22. Teshima, M. (2001), private communication. To show the data of AGASA and Akeno we reduced the energies of AGASA by 10%, as recommended in Nagano, M. and Watson, A., *Rev. of Mod. Phys.* **72**, 689.
23. Stecker, F., and Salamon, M. (1999), *Ap. J.*, **512**, 521.
24. Olinto, A. (2000) astro-ph/0011106.
25. Kifune, T. (1999) *ApJ*, Vol. 518, p. L21.
26. Amelio-Camelia, G., et al. (1998) *Nature*, Vol. 393, p. 763.
27. <http://owl.gsfc.nasa.gov>